Microheterogeneity and Microrheology of Wheat Gliadin Suspensions Studied by Multiple-Particle Tracking

Jingyuan Xu,[†] Yiider Tseng,[‡,§] Craig J. Carriere,[†] and Denis Wirtz*[,‡,§,||]

Biomaterials Processing Research, National Center for Agricultural Utilization Research, Agricultural Research Service, United States Department of Agriculture, Peoria, Illinois 61604, and Department of Chemical Engineering, Graduate Program in Molecular Biophysics, and Department of Materials Science and Engineering, The Johns Hopkins University, Baltimore, Maryland 21218

Received July 16, 2001; Revised Manuscript Received October 12, 2001

By monitoring the thermally driven displacements of imbedded polystyrene microspheres via video fluorescence microscopy, we quantified the microstructural and micromechanical heterogeneities of wheat gliadin suspensions. We found that the degree of heterogeneity of the suspensions, as measured by the width and skewness of the microspheres' mean squared displacement (MSD) distribution, increased dramatically over a narrow range of gliadin concentrations. The ensemble-averaged MSD of a 250 mg/mL gliadin suspension exhibited a power-law behavior scaling linearly with time, a behavior similar to that observed for a homogeneous aqueous glycerol solution. However, the MSD distribution was wider and more asymmetric than for glycerol. With increasing concentration of gliadin, the ensemble-averaged MSD rapidly displayed a plateau at small time scales, the MSD distribution became wider and more asymmetric, and the local viscoelastic moduli extracted from multiple-particle-tracking measurements showed an increasingly wide range.

Introduction

We report a quantitative study of the micromechanical and microstructural properties of wheat gliadin suspensions. We use the recently introduced multiple-particle-tracking (MPT) method, which simultaneously monitors the displacements of a large number of individual microspheres, to quantify the degree of heterogeneity of gliadin suspensions from the distributions of the microspheres' mean squared displacements. More traditional approaches that probe the spatial heterogeneity of gels and networks either provide qualitative insight or "ensemble-average" local properties. Electron microscopy (EM) has successfully been used to obtain detailed (microscopic) structural information on macromolecular assemblies, filamentous proteins, and polymers via computer-aided image reconstruction. However, EM cannot provide an unbiased view of the polymer ultrastructure in solution (i.e., pore distribution, etc.), and it often requires harsh staining procedures.[1,2] Cryo-electron microscopy preserves the three-dimensional organization of a polymer network but has not been extended to quantify the heterogeneities of networks.[3] Confocal microscopy can image the three-dimensional architecture of a network[4] but uses fluorescent dyes that can affect intermolecular interactions and does not provide a quantitative marker for comparing the heterogeneity of different complex fluids. Light-scattering spectra can be used to estimate the mesh size of a polymer network indirectly, but this technique poses problems of multiple scattering at large polymer concentration and provides only ensemble-averaged microstructural information.[4,5] Rheology, which measures the in- and out-of-phase responses of a fluid to an applied stress or deformation, is intimately related to the microstructure of the fluid.[6] However, inferring structural information from rheological data is an inverse problem that typically has more than one solution.[7] Diffusing wave spectroscopy (DWS), which has been used extensively to test the dynamics of biopolymers in solution,[8−12] probes a much wider range of frequencies than rheology without resorting to the temperature-superposition approach.[6] DWS, however, monitors the Brownian motion of thousands of particles simultaneously and, therefore, completely loses statistical (i.e., distribution) and spatial information about the tested network.

Multiple-particle tracking does not require staining agents, preserves the three-dimensional character of the network, and yields parameters that quantify the degree of heterogeneity of complex fluids.[13−15] MPT monitors the thermally driven displacements of a large number of probe particles individually and simultaneously. Statistical analysis of the distributions of mean squared displacements leads to relative markers that can be compared to those of other complex fluids. Here, we show that MPT provides novel, quantitative insight into the microstructure and microrheology of networks of gliadin proteins.

* Corresponding author: Denis Wirtz, Ph.D. Department of Chemical Engineering, The Johns Hopkins University, 3400 North Charles Street, Baltimore, MD 21218. Phone: 410-516-7006. Fax: 410-516-5510. E-mail: wirtz@jhu.edu.

[†] United States Department of Agriculture.

[‡] Department of Chemical Engineering, The Johns Hopkins University.

[§] Graduate Program in Molecular Biophysics, The Johns Hopkins University.

[||] Department of Materials Science and Engineering, The Johns Hopkins University.

10.1021/bm015586b CCC: $22.00 © 2002 American Chemical Society
Published on Web 11/22/2001

The superfamily of gliadin proteins is composed of at least 50 members, which all contain extensive intramolecular disulfide bonding. Primary sequences of gliadins are rich in glutamine and proline residues (~35 and 20%, respectively) but contain few basic and acidic amino acids.[16] Along with glutenin, gliadin is one of the major constituents of wheat gluten, the ingredient responsible for the viscoelastic properties of dough.[17] The unique physical and biochemical properties of gluten make it suitable for numerous nonfood applications. Gluten has recently been exploited in engineering new types of biodegradable plastics and biomaterials for applications in drug delivery, tissue engineering, and the environment. It is known that gliadin contributes extensibility and viscosity,[18,19] underlying the important role of gliadin in governing the end-use quality of wheat.[20−25] However, the structure−function relationship of gliadin is still not clearly understood. Here, we apply multiple-particle tracking to systematically interrogate the local microstruture and micromechanical properties of gliadin suspensions.

Methods and Materials

Materials and Sample Preparation. The wheat gliadin used in this study was donated by Dr. O. Maningat of Midwest Grain Products, Inc. (Atchison, Kansas). It contained a minimum of 75% gliadin protein, 1.0−2.0% ash, 5.0−8.0% moisture, and 1.0−2.0% fat, as well as a maximum of 1.0% fiber. Wheat gliadin was used as received and was suspended in a 0.05 M pH 7.0 (25 °C) sodium phosphate buffer containing 3 M urea via extensive mixing by using a stirrer.[26] These buffer conditions allow the gliadin to be dissoved in water but remain mild for gliadin, as documented in refs 27−29. Gliadin seemed well-dispersed as crudely assessed by light microscopy, and no sedimentation occurred during 2 weeks after sample preparation. Samples were stored at 4 °C and used within 4 days after preparation to avoid sample degradation. At least two samples were analyzed for each tested gliadin concentration.

For a control, we selected glycerol because it is a viscous liquid (i.e., its elastic modulus is 0) that has a nominal shear viscosity of 1 P, which is close to that of the gliadin solutions tested here. Moreover glycerol is perfectly homogeneous, at least at length scales much smaller than the radius of the microspheres selected for the MPT experiments.

Multiple-Particle Tracking (MPT). To quantify the degree of structural and mechanical microheterogeneity of gliadin suspensions, we used the method of multiple-particle tracking (MPT), which was originally described by Apgar et al.[13] The principle of MPT consists of monitoring the thermally driven motion of inert microspheres that are evenly distributed within the solutions and to statistically analyze their displacement distributions, from which information about the extent of heterogeneity can be extracted. For each experiment, a dilute, well-dispersed suspension of 0.97-μm-diameter, fluorescent polystyrene microspheres (0.1 vol %) was gently mixed with the gliadin suspension. The mixture containing the gliadin suspension and the probe microspheres (total volume of ~0.3 mL) was deposited into a PC20 CoverWell cell (Grace Bio-Lab, Eugene, OR), which was placed on the stage of a light microscope and allowed to equilibrate for at least 2 h at room temperature ($T \approx 295$ K). Images of the fluorescent beads were recorded onto the (large) random-access memory of a PC computer via a silicon-intensifier target (SIT) camera (VE-100 Dage-MTI, Michigan City, IN) mounted on an inverted epifluorescence microscope (Eclipse TE300, Nikon, Melville, NY).[30] A 100×, 1.3 numerical aperture, oil-immersion lens was used for the measurements, which permitted ~5-nm spatial resolution, as assessed by monitoring the apparent displacements of the microspheres firmly attached to a glass coverslip identical to that of the bottom of the CoverWell cell with the same microscope and camera settings as used during the experiments with gliadin solutions.

Movies of fluctuating microspheres were analyzed by a custom MPT routine incorporated into the software Metamorph (Universal Imaging Corp., West Chester, PA) as described in refs 13 and 15. The displacements of the particles centroids were simultaneously monitored in a 120 μm × 120 μm field of view for 120 s at a rate of 30 Hz. Between 10 and 30 individual particles were tracked, a number that was determined by balancing potential particle−particle interactions at high particle density with the tracking of a sufficiently large number of beads per movie, but was not limited by the tracking capabilities of our microscope/software/computer system. For each tested gliadin suspension, we tracked a total of ~240 microspheres. Individual time-averaged mean squared displacements (MSD), $\langle \Delta r^2(\tau) \rangle = \langle [x(t+\tau) - x(t)]^2 + [y(t+\tau) - y(t)]^2 \rangle$, where τ is the time lag and t is the elapsed time, were calculated from the two-dimensional coordinates, (x, y), of the particles centroids. The MSD of a microsphere has a convenient physical interpretation as it is proportional to the local compliance, $\Gamma(\tau) = (\pi a/k_B T)\langle \Delta r^2(\tau) \rangle$, of the specimen due to the small, local random force created by the fluctuating microsphere.[8] Here, k_B is the Boltzmann constant, T is the absolute temperature of the specimen, and a is the radius of the probe microsphere. From $\langle \Delta r^2(\tau) \rangle$ data, time-lag-dependent ensemble-averaged MSD, $\langle\langle \Delta r^2(\tau) \rangle\rangle$, and MSD distributions were computed (see Results and Discussion).

Local frequency-dependent elastic moduli $G'(\omega)$ and loss moduli $G''(\omega)$ were computed from individual MSD traces as described in refs 10 and 11. Neglecting inertial effects and assuming that the fluid surrounding the probe particles is incompressible, the viscoelastic spectrum $G(s)$, which is derived from a generalized Langevin equation for the motion of the microsphere, is

$$G(s) = k_B T/\pi a s \langle \Delta r^2(s) \rangle$$

Here, s is the Laplace frequency and $\langle \Delta r^2(s) \rangle$ is the unilateral Laplace transform of $\langle \Delta r^2(\tau) \rangle$. The elastic modulus $G'(\omega)$ and loss modulus $G''(\omega)$ are the real and imaginary parts, respectively, of the complex viscoelastic modulus $G_d(\omega)$, which is the projection of $G(s)$ in Fourier space.[10,11] This formalism holds as long as the size of the probe microspheres is much larger than the characteristic mesh size of the solution, which is the case in the present study.

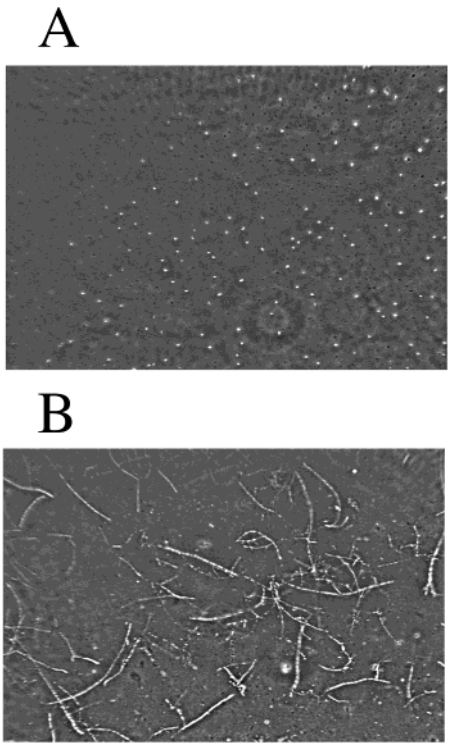

Figure 1. Phase-contrast micrographs of gliadin solutions. (A) 250 mg/mL, (B) 400 mg/mL. The bottom border of each image represents 1000 μm.

For gliadin suspensions, most of the measurements were conducted using beads of 0.97-μm diameter, some with beads of 0.50-μm diameter. Whereas the measured MSDs were sensitive to bead size (via the diffusion coefficient) as expected, the shape of the MSD distribution was not size-dependent. We also used the relative bin distribution as a marker of heterogeneity, which does not depend on bead size (see Results section). This bin distribution is not sensitive to the actual mean of the MSD and depends only on the heterogeneity of the tested specimen.

Light Microscopy. Phase-contrast microscopy was used to assess the microstructure of gliadin suspensions qualitatively. Images were collected with a CCD camera mounted on an inverted light microscope via a 20×-magnification lens (Nikon).

Results and Discussion

Microstructural Heterogeneities of Gliadin Suspensions: Effect of Concentration. Gross microstructural properties of gliadin solutions were detected using phase-contrast microscopy (Figure 1). Low-concentration gliadin suspensions were featureless (Figure 1A), but the high concentration displayed elongated fibers (Figure 1B). Here, light microscopy illustrates well this concentration-induced transition in gliadin solutions, but neither provides quantitative markers describing the solution microstructure nor directly yields physical properties of the solutions. To quantify micromechanical and microstructural properties of wheat gliadin suspensions, the thermally driven motion of a large collection of 0.97 μm-diameter polystyrene beads embedded in suspensions of various gliadin concentrations was tracked with ~5-nm resolution at a rate of 30 Hz via time-resolved video fluorescence microscopy. Typical trajectories of microspheres dispersed in suspensions of increasing gliadin concentration are shown in Figure 2. The extent of the displacements (measured at various time scales) was greatly reduced with increasing gliadin concentration (Figure

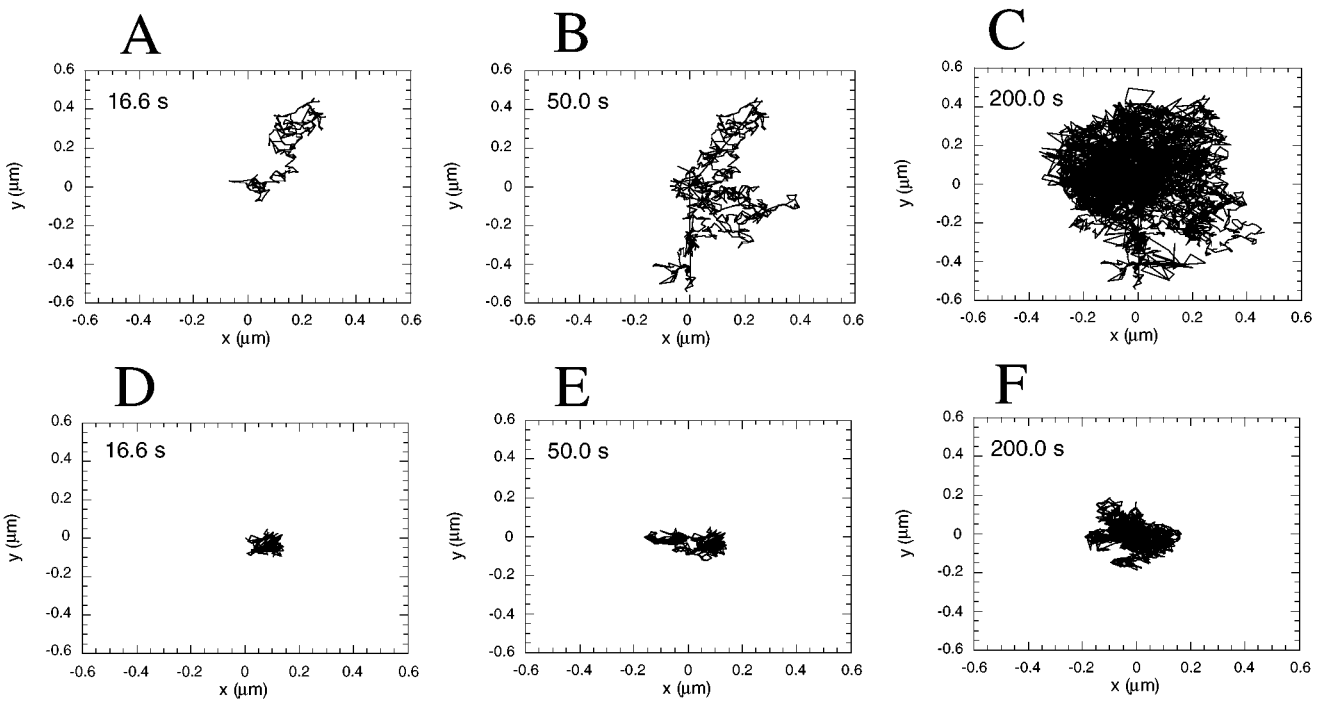

Figure 2. Typical trajectories of a 0.97-μm-diameter, fluorescent polystyrene microsphere embedded in a wheat gliadin suspension. Two-dimensional trajectories of the centroid of a single microsphere (A−C) in a 250 mg/mL gliadin suspension and (D−F) in a 400 mg/mL gliadin suspension. The thermally driven motion of the bead was recorded for (A, D) 16.6 s, (B, E) 50 s, and (C, F) 200 s. The trajectory was captured with a spatial resolution of ~5 nm and a temporal resolution of 33 ms by monitoring the bead's intensity-weighted centroid displacement via time-lapsed video fluorescence microscopy and a multiple-particle-tracking software (see Methods and Materials).

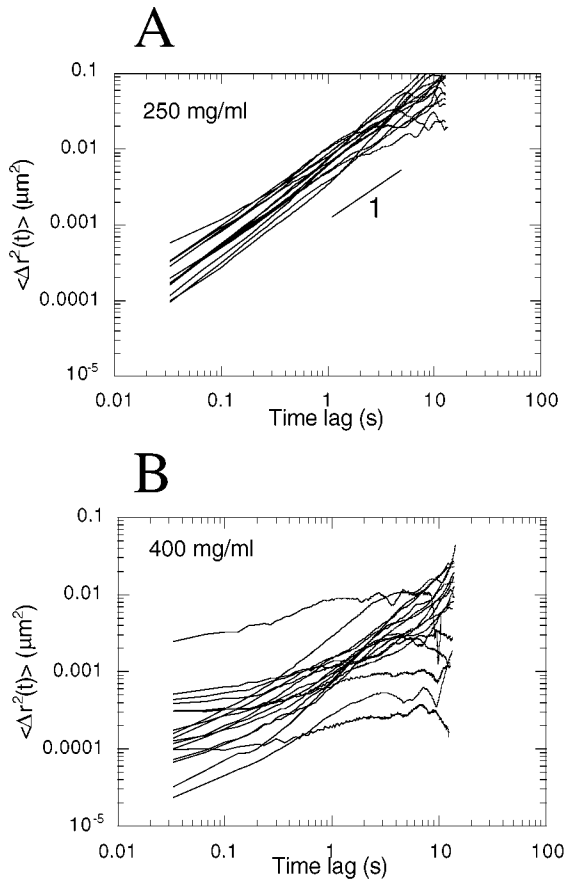

Figure 3. Mean squared displacements of individual microspheres dispersed in wheat gliadin suspensions. Randomly selected mean squared displacement (MSD) as a function of time lag for suspensions containing (A) 250 mg/mL and (B) 400 mg/mL gliadin.

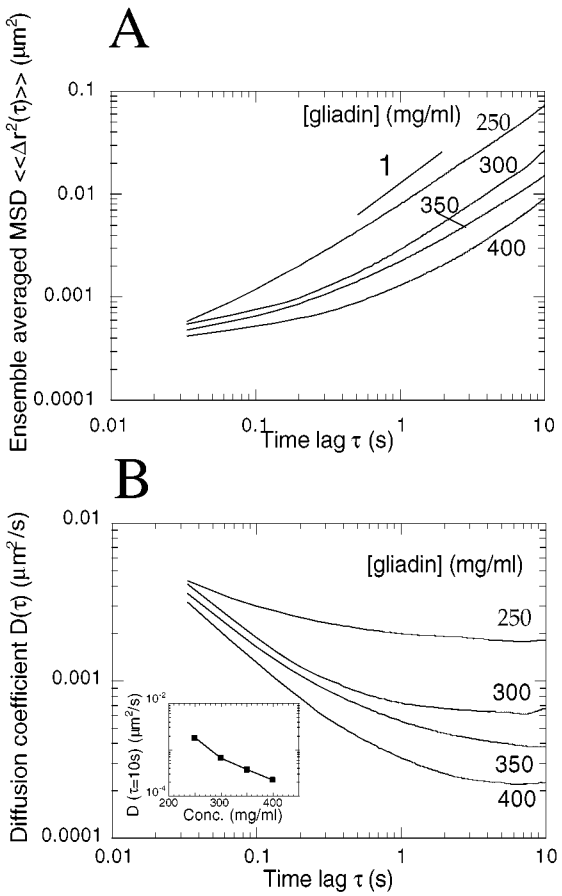

Figure 4. Ensemble-averaged mean squared displacement (MSD) and diffusion coefficient of beads imbedded in wheat gliadin suspensions. (A) Time-dependent ensemble-averaged MSD, $\langle\langle \Delta r^2(\tau)\rangle\rangle$, which was obtained by summing measured MSDs divided by the number of probed particles for various gliadin concentrations ($n \approx 240$). (B) Time-dependent ensemble-averaged diffusion coefficient, $D(\tau)$. Inset: Diffusion coefficient measured at a time scale of 10 s as a function of gliadin concentration.

2), a result that parallels the fact that wheat gliadin suspensions of high concentration exhibit high viscosity[26] (see more below).

Coordinates of the particles' centroids were transformed into mean squared displacement (MSD) traces and statistically analyzed. For a 250 mg/mL gliadin concentration, a majority of MSD traces adopted a power-law behavior as a function of time scale with a slope close to unity over most of the probed range of time scales (Figure 3A). This result suggests that probe microspheres underwent purely diffusive motion in a material with a viscous liquid character, for which one would predict $\langle \Delta r^2(\tau)\rangle \sim \tau$. At higher gliadin concentrations, however, the displacements of microspheres at different locations within the suspension displayed a wide range of amplitudes and time scale dependences (Figure 3B). The amplitude of MSD traces of microspheres imbedded in high-concentration solutions was lower than those for low gliadin concentrations. A majority of MSD traces were weakly dependent on time scale, a subdiffusive behavior ($\langle \Delta r^2(\tau)\rangle \sim \tau^\alpha$ with $\alpha < 1$) that is a signature of "elastic trapping" of the beads by the mesh of the gliadin solution (Figure 3B).[31,32]

To derive properties that describe the macroscopic behavior of gliadin suspensions, the ensemble-averaged MSD and ensemble-averaged diffusion coefficient were calculated from the individual MSD traces of a large ensemble of microspheres ($n = 240$). For a 250 mg/mL gliadin suspension, the ensemble-averaged MSD showed a power-law behavior over most of the probed time scale range, with a slope close to unity at time scales slower than ~0.2 s (Figure 4A). Accordingly, the ensemble-averaged diffusion coefficient of the microspheres, $D(\tau) = \langle\langle \Delta r^2(\tau)\rangle\rangle/4\tau$, decreased slightly from 3.0×10^{-3} μm^2/s at a time scale of 0.1 s to 1.8×10^{-3} μm^2/s at 10 s (Figure 4B). By comparison, the same microsphere has a constant diffusion coefficient of 0.4 μm^2/s in water ($k_BT/6\pi\eta a$, with viscosity $\eta \approx 0.01$ P at a temperature of $T = 295$ K) and 4.2×10^{-3} μm^2/s in glycerol (computed from MSD data in Figure 7, see below). The 400 mg/mL suspension showed a quasi plateau at small time scales and an upturn for time scales larger than ~0.5 s. This upturn describes the relaxation dynamics of the fluid surrounding the probe microspheres, which results in beads translocating from a local elastic trap to a neighboring one within the solution (Figure 4A). At 400 mg/mL, the diffusion coefficient was small and decreased strongly with time scale, from 13.0×10^{-4} μm^2/s at 0.1 s to 2.2×10^{-4} μm^2/s at 10 s (Figure 4B). At intermediate concentrations, the amplitudes of the ensemble-averaged MSDs and diffusion coefficients were intermediate. The time scale dependences of the diffusion coefficient and the ensemble-averaged MSD were

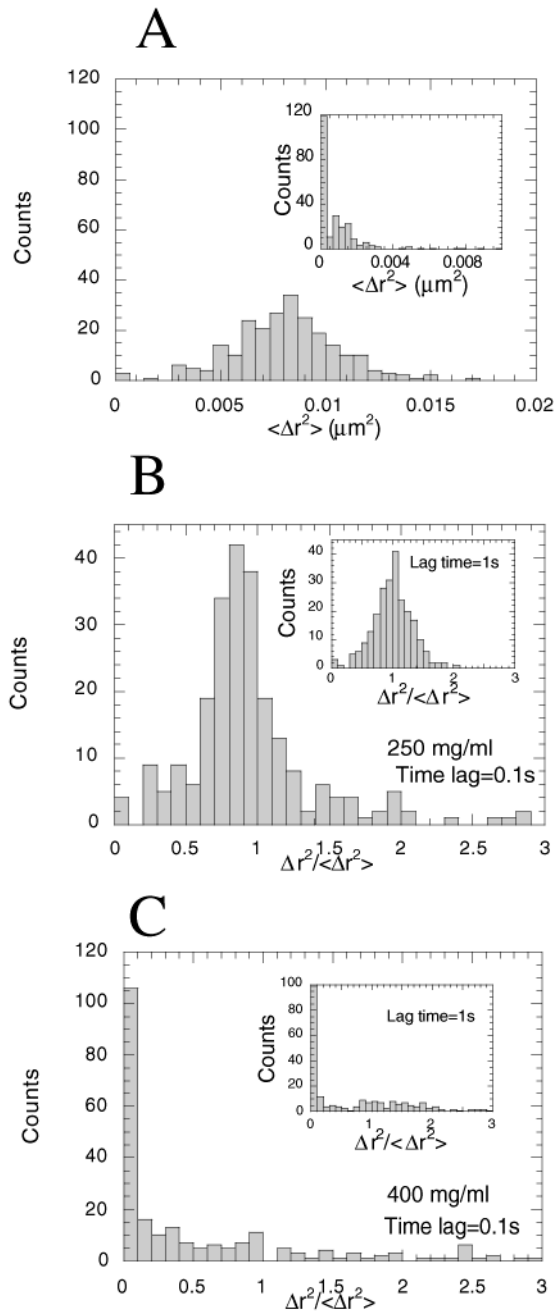

Figure 5. Mean squared displacement (MSD) distributions. (A) MSD distributions measured at a time lag of 0.1 s for a gliadin concentration of 250 mg/mL. Inset: MSD distribution for a 400 mg/mL gliadin suspension. MSD distributions measured at a time lag of 0.1 s, normalized by the corresponding ensemble-averaged mean (taken from Figure 3) for gliadin concentrations of (B) 250 mg/mL and (C) 400 mg/mL. Insets in B and C: Normalized MSD distributions measured at a time lag of 1 s.

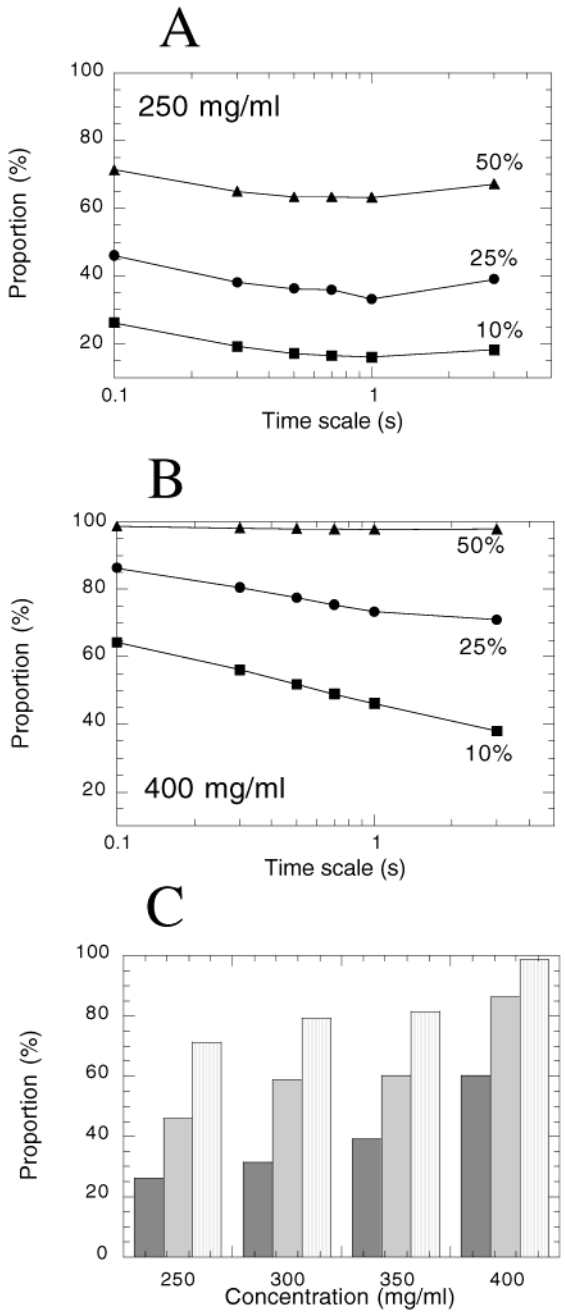

Figure 6. Statistical analysis of MSD distributions in gliadin suspensions. Time-dependent contributions (in %) of the 10, 25, and 50% highest MSD values to the ensemble-averaged MSD for gliadin concentrations of (A) 250 mg/mL and (B) 400 mg/mL. (C) Contributions of the 10% (first column), 25% (second column), and 50% (third column) highest MSD values to the ensemble-averaged MSD at a time scale of 0.1 s as a function of gliadin concentration. The larger these contributions, the more heterogeneous the MSD distribution, and therefore, the more heterogeneous the gliadin suspension.

also intermediate between those of the 250 and 400 mg/mL solutions (Figure 4, A and B). The diffusion coefficient, measured at long time scales, decreased extremely rapidly (about exponentially) over a small range of gliadin concentrations (Figure 4B, inset).

To quantify the level of heterogeneity in the gliadin suspensions, MSD distributions were generated from the MSD traces and statistically analyzed. As a control, the same analysis was applied to an aqueous solution of glycerol, which is homogeneous at length scales at least as small as the bead radius ($\sim$0.5 μm). For the 250 mg/mL gliadin suspension, MSD distributions were relatively symmetric about the mean (Figure 5A). In the case of the 400 mg/mL suspension, a vast majority of the MSD values were close to the mean ($\sim 4 \times 10^{-3}$ μm^2), but extreme values appeared that were an order of magnitude larger than the mean. To further compare the gliadin suspensions, MSD distributions were normalized by the ensemble-averaged MSD (Figure 5, B and C). For a 250 mg/mL suspension and at a time scale

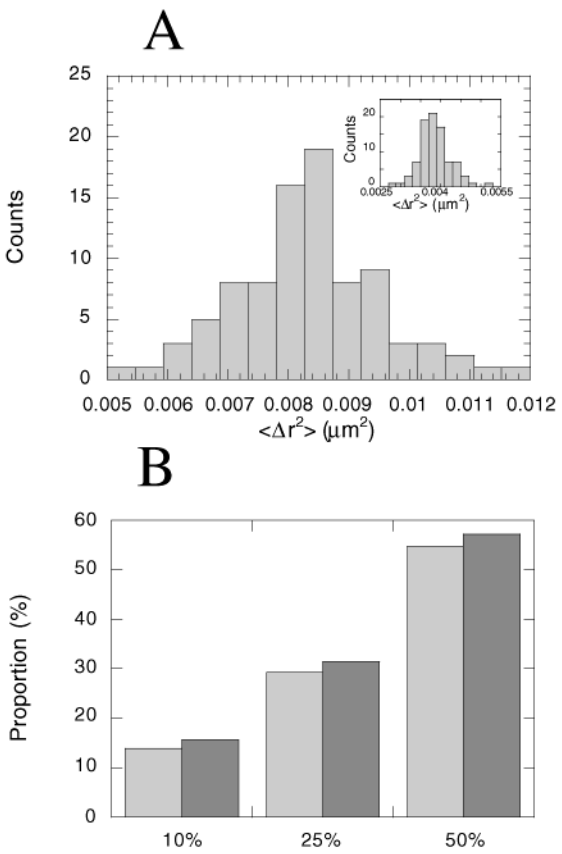

Figure 7. Statistical analysis of the MSD distribution in an aqueous glycerol solution. (A) MSD distribution at a time lag of 0.1 s. Inset: MSD distribution at a time lag of 1.0 s. (B) Contributions (in %) of the 10, 25, and 50% highest MSD values to the ensemble-averaged MSD at a time scale of 0.1 s (first column) and 1.0 s (second column). Note that the contributions are close to those predicted for a perfectly homogeneous solutions, which should be exactly 10, 25, and 50%, respectively.

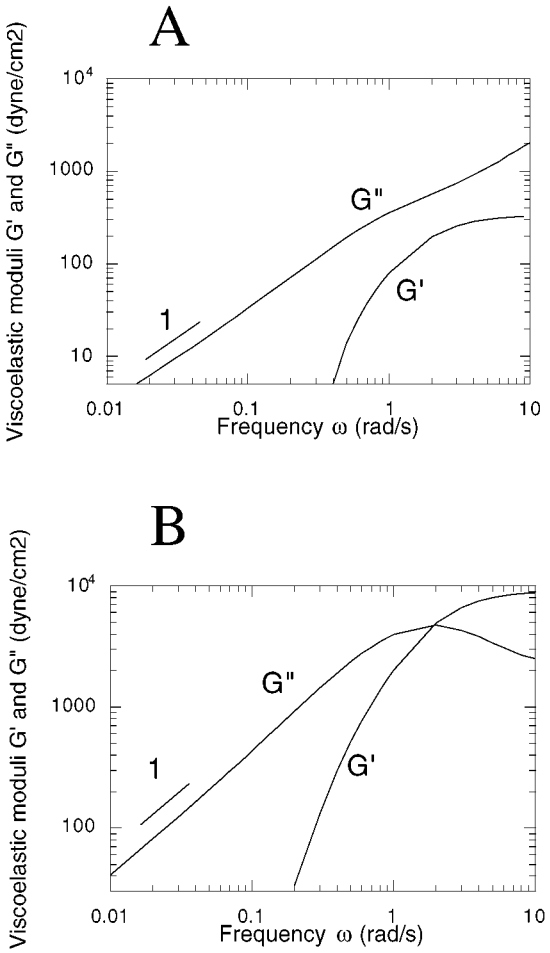

Figure 8. Micromechanical properties of gliadin suspensions. Ensemble-averaged, frequency-dependent elastic modulus and viscous modulus of (A) 250 mg/mL and (B) 400 mg/mL gliadin suspensions.

of 1 s, the normalized median, standard deviation, and skewness were 1.01, 0.32, and 0.35, respectively. These statistical parameters, which were directly extracted from the MSD distributions, are similar to those observed with an aqueous solution of glycerol, which is (theoretically) perfectly homogeneous. Indeed, the standard deviation, median, and skewness of the MSD distribution at a time scale of 1 s for beads dispersed in glycerol were 1.02, 0.15, and 0.39, respectively. The shape of the MSD distribution of the 250 mg/mL suspension was relatively independent of time scale (Figure 5, B and C, insets); so was the MSD distribution for the homogeneous glycerol solution (Figure 7A, inset, and Figure 7B).

Nevertheless, by analyzing the contributions of the 10, 25, and 50% highest MSD values to the ensemble-averaged MSD at a given time scale, we found that the glycerol solution was more homogeneous than the 250 mg/mL suspension (Figures 6 and 7B). For glycerol, these parameters were indeed close to those expected for a perfectly homogeneous liquid (10, 25, and 50%) (Figure 7B), for which all MSD values should theoretically be similar. In contrast, for the 250 mg/mL suspension, these parameters were typically twice as large as those observed in glycerol over the same range of time scales (Figures 6A and 7B). Therefore, despite the fact that a 250 mg/mL gliadin suspension behaved mostly like a liquid from a macroscopic standpoint (Figure 4A), that suspension displayed a much higher degree of heterogeneity than the homogeneous glycerol solution.

The 400 mg/mL suspension displayed a MSD distribution that was wide and highly skewed (Figure 5C). Moreover, the shape of the MSD distribution was highly dependent on time scale: relatively narrow and symmetric at short time scales vs wide and skewed at long time scales. At a time scale of 1 s, the median of the normalized MSD distribution was much smaller (0.34) and the standard deviation and skewness were much larger (1.61 and 1.36, respectively) than those observed in the 250 mg/mL suspension and glycerol. Furthermore, the contributions of the 10, 25, and 50% highest MSD values to the ensemble-averaged MSD were larger than those of the more dilute gliadin suspension (Figure 6, B and C) and much larger than 10, 25, and 50%, which are the values predicted for a homogeneous solution.

The transition between the liquidlike behavior of gliadin suspensions at low concentrations and the highly heterogeneous solidlike behavior at high concentrations occurred over a narrow range of concentrations (Figure 4). We studied the amplitude of the MSD and the shape of the MSD distributions at intermediate concentrations. The slope of the curve of the ensemble-averaged MSD vs time lag deviated from unity at progressively earlier time scales with increasing

gliadin concentration (Figure 4A). The mean diffusion coefficient dropped rapidly with gliadin concentration (Figure 4B). The MSD distributions became progressively asymmetric and broad with increasing concentration (data not shown): the contributions of the 10, 25, and 50% highest MSD values to the ensemble-averaged MSD increased rapidly with increasing gliadin concentration (Figure 6C). This indicates that the degree of heterogeneity in gliadin suspensions was much higher than in viscous liquids such as water and glycerol and that it increased greatly with gliadin concentration.

Micromechanical Heterogeneities of Gliadin Suspensions. The local mechanical properties of gliadin suspensions were extracted from MSD measurements following Mason et al.'s method[10] (see Methods and Materials). After unilateral Laplace transformation of each lag-dependent MSD trace, a complex modulus was calculated, from which frequency-dependent elastic and viscous moduli, $G'(\omega)$ and $G''(\omega)$, respectively, were extracted (Figure 8, A and B). We found that the 250 mg/mL suspension exhibited a nonnegligible elasticity only at high frequencies, and a viscous modulus that increased almost linearly with frequency, a signature of mostly liquidlike behavior (Figure 8A). The local viscosity (measured at 1 rad/s) ranged between 4 and 34 P about a mean of 22 P (1 P = 1 Poise = 10^{-1} N s/m^2; viscosity of water is ~0.01 P). This represented a variation significantly wider than that measured in glycerol solutions, for which the viscosity ranged between 0.92 and 1.08 P (nominal viscosity of 1 P). The 400 mg/mL suspension showed a significant degree of elasticity at high frequencies but remained a viscoelastic liquid, for which $G''(\omega) > G'(\omega)$, over most of the frequency range ($0.1 < \omega < 10$ rad/s) (Figure 8B).

Conclusions

Wheat proteins, such as gluten, glutenin, and gliadin, have recently attracted much interest from researchers because of their unique properties suitable to food processing and nonfood applications.[33] However, the understanding of structure−function relationship of solutions of these proteins is still extremely limited. Some researchers believe that glutenin mainly controls the properties of gluten and that gliadin acts only as a dilutant.[34−36] Other researchers have suggested that gliadin plays an important role in governing the mechanical function of gluten.[20−25] In this work, we studied the micromechanical and microstructural properties of gliadin suspensions using the multiple-particle-tracking method. One of the outcomes of this work was the detection of a relatively rapid concentration-induced transition of the mechanical properties of the gliadin suspensions. Pretransitional effects were apparent at low concentrations, as clearly detected by the shape of the MSD distribution of imbedded particles. Whereas the overall ensemble-averaged MSD was very similar in shape to that of a viscous liquid, the viscosity distribution was much wider than that measured in a (homogeneous) glycerol solution. Another outcome of this study was the establishment of a framework for studying the structure−function relationship of gels and networks. By extracting *relative* markers, such as the standard deviation, skewness, median, and bin distribution from normalized and nonnormalized MSD and moduli distributions, the heterogeneity in the mechanical and structural properties of very different complex fluids can be directly compared. These complex fluids can be as varied as the cytoskeleton of a living cell,[37] DNA solutions in the presence/absence of DNA-binding enzymes,[10,38] reconstituted actin filament networks,[13,15,39] keratin filament suspensions,[14,40] and genetically engineered protein gels for drug delivery applications.[41]

Acknowledgment. D.W. and Y.T. acknowledge financial support from the NSF (CTS9812624 and CTS0072278). Names are necessary to report factually on available data; however, the USDA neither guarantees nor warrants the standard of the product, and the use of the name by the USDA implies no approval of the product to the exclusion of others that may also be suitable.

References and Notes

(1) Depriester, W. *Electron Microsc. Rev.* **1991**, *4*, 343−376.
(2) Schoenenberger, C. A.; Steinmetz, M. O.; Stoffler, D.; Mandinova, A.; Aebi, U. *Microsc. Res. Tech.* **1999**, *47*, 38−50.
(3) Jarnik, M.; Aebi, U. *J. Struct. Biol.* **1991**, *107*, 291−308.
(4) Tseng, Y.; Fedorov, E.; McCaffery, J. M.; Almo, S. C.; Wirtz, D. *J. Mol. Biol.* **2001**, *310*, 351−366.
(5) Chu, B. *Laser Light Scattering: Basic Principles and Practice*, 2nd ed.; Academic Press: New York, 1991.
(6) Ferry, J. D. *Viscoelastic Properties of Polymers*; John Wiley and Sons: New York, 1980.
(7) Doi, M.; Edwards, S. F. *The Theory of Polymer Dynamics*; Clarendon Press: Oxford, 1986.
(8) Xu, J.; Viasnoff, V.; Wirtz, D. *Rheol. Acta* **1998**, *37*, 387−398.
(9) Palmer, A.; Cha, B.; Wirtz, D. *J. Polym. Sci. B: Polym. Phys.* **1998**, *36*, 3007−3015.
(10) Mason, T. G.; Ganesan, K.; van Zanten, J. V.; Wirtz, D.; Kuo, S. C. *Phys. Rev. Lett.* **1997**, *79*, 3282−3285.
(11) Xu, J.; Palmer, A.; Wirtz, D. *Macromolecules* **1998**, *31*, 6486−6492.
(12) Rufener, K.; Palmer, A.; Xu, J.; Wirtz, D. *J. Non-Newtonian Fluid Mech.* **1999**, *82*, 303−314.
(13) Apgar, J.; Tseng, Y.; Federov, E.; Herwig, M. B.; Almo, S. C.; Wirtz, D. *Biophys. J.* **2000**, *79*, 1095−1106.
(14) Ma, L.; Yamada, S.; Wirtz, D.; Coulombe, P. A. *Nat. Cell Bio.* **2001**, *3*, 503−506.
(15) Tseng, Y.; Wirtz, D. *Biophys. J.* **2001**, *81*, 1643−1656.
(16) Cornell, H. J.; Hoveling, A. W. *Wheat−Chemistry and Utilization*; Technomic Publishing Co. Inc.: Lancaster, PA, 1998.
(17) MacRichie, F. *Adv. Food Nutr. Res.* **1992**, *36*, 1−85.
(18) Ciaffi, M.; Tozzi, L.; Lafiandra, D. *Cereal Chem.* **1996**, *73*, 346−351.
(19) Wall, J. S. In *Recent Advances in Biochemistry of Cereals*; Laidman, D. L., Wyn-Jones, R. G., Eds.; Academic Press: London, 1979; pp 275−311.
(20) Preston, K.; Woodbury, W.; Bendelow, V. *Cereal Chem.* **1975**, *52*, 427−430.
(21) Branlard, G.; Dardevet, M. *J. Cereal Sci.* **1985**, *3*, 329−343.
(22) van Lonkhuijsen, H. J.; Hamer, R. J.; Schreuder, C. *Cereal Chem.* **1992**, *69*, 174−177.
(23) Huebner, F. R.; Bietz, J. A. *Cereal Chem.* **1993**, *70*, 506−511.
(24) Hou, G.; Yamamoto, H.; Ng, P. K. W. *Cereal Chem.* **1996**, *73*, 352−357.
(25) Hussain, A.; Lukow, O. M. *Cereal Chem.* **1997**, *74*, 791−799.
(26) Xu, J.; Bietz, J. A.; Felker, F. C.; Carriere, C. J.; Wirtz, D. *Cereal Chem.* **2001**, *78*, 181−185.
(27) Wu, Y. V.; Dimler, R. J. *Arch. Biochem. Biophys.* **1964**, *107*, 435−440.
(28) Ewart, J. A. *J. Sci. Food Agric.* **1980**, *31*, 1323−1336.
(29) Bietz, J. A. *Baker's Dig.* **1984**, *58*, 15−17.
(30) Leduc, P.; Haber, C.; Bao, G.; Wirtz, D. *Nature* **1999**, *399*, 564−566.

(31) Amblard, F.; Maggs, A. C.; Yurke, B.; Pargellis, A. N.; Leibler, S. *Phys. Rev. Lett.* **1996**, *77*, 4470−4473.
(32) Palmer, A.; Xu, J.; Kuo, S. C.; Wirtz, D. *Biophys. J.* **1999**, *76*, 1063−1071.
(33) Cuq, B.; Gontard, N.; Guilbert, S. *Cereal Chem.* **1998**, *75*, 1−9.
(34) Payne, P. I.; Corfield, K. G.; Blackman, J. A. *Theor. Appl. Genet.* **1979**, *55*, 153−159.
(35) Chakraborty, K.; Khan, K. *Cereal Chem.* **1988**, *65*, 340−344.
(36) Weegels, P. L.; Marseille, J. P.; Bosveld, P.; Hamer, R. J. *J. Cereal Sci.* **1994**, *20*, 253−264.
(37) Yamada, S.; Wirtz, D.; Kuo, S. C. *Biophys. J.* **2000**, *78*, 1736−1747.
(38) Mason, T. G.; Dhople, A.; Wirtz, D. In *Statistical Mechanics in Physics and Biology*; Wirtz, D., Halsey, T. C., Eds.; Materials Research Society: Warrendale, PA, 1997; pp 153−158.
(39) Gittes, F.; Schnurr, B.; Olmsted, P. D.; MacKintosh, F. C.; Schmidt, C. F. *Phys. Rev. Lett.* **1997**, *79*, 3286−3289.
(40) Coulombe, P. A.; Bousquet, O.; Ma, L.; Yamada, S.; Wirtz, D. *Trends Cell Biol.* **2000**, *10*, 420−428.
(41) Petka, W. A.; Harden, J.; McGrath, K. P.; Wirtz, D.; Tirrell, D. A. *Science* **1998**, *281*, 389−393.

BM015586B